ELSEVIER

Journal of Biomechanics 35 (2002) 673–681

JOURNAL OF BIOMECHANICS

www.elsevier.com/locate/jbiomech
www.JBiomech.com

Computer simulations of mitosis and interdependencies between mitosis orientation, cell shape and epithelia reshaping

G. Wayne Brodland*, Jim H. Veldhuis

Department of Civil Engineering, University of Waterloo, Waterloo, Ont., Canada N2L 3G1

Accepted 28 December 2001

Abstract

Finite element-based computer simulations are used to investigate mitosis and how mitosis, cell shape, and epithelium reshaping depend on each other. Frame- and cell-oriented patterns of mitosis with growing and non-growing daughter cells are considered. Previous simulations have shown that applied stresses or strains can reshape cells so that their long axes are aligned in the principal stretch direction. The simulations reported here show that this can produce global alignment of the mitosis cleavage planes. Other simulations reported here show that mitoses with suitably aligned cleavage planes can drive epithelium reshaping. Formulas that quantify these and other dependencies are derived. These formulas provide quantitative relationships against which current hypotheses regarding epithelia reshaping in real biological systems can be evaluated.

Keywords: Cell mechanics; Mitosis; Cell shape; Epithelia; Epithelium reshaping; Oriented mitosis; Finite element method; Computer simulations; Fabric

1. Introduction

As the cells in an epithelium divide, reshape, and rearrange, they cause the epithelium to undergo in-plane growth, shrinkage, elongation and out-of-plane bending (Sausedo et al., 1997; Clausi and Brodland, 1993; Burnside and Jacobson, 1968), and thereby drive critical components of processes ranging from embryogenesis to wound healing (Kalnins et al., 1995; Shimizu et al., 1995; Hertzler and Clark, 1992; Schoenwolf and Alvarez, 1989). In spite of these diverse roles, epithelia share important biochemical, morphological and mechanical features (Fenteany et al., 2000).

One of these features is that the cells of which they are made undergo autonomous repeated divisions (Fig. 1). Although a primary function of mitosis is to bring about cell proliferation, it can also produce daughter cells that are functionally different from each other (Way et al., 1994; Lydon, 1990; Watt and Smith, 1989), and has been hypothesized to drive autonomous reshaping of epithelia (Zhao et al., 1999; Sausedo et al., 1997; Beebe and Masters, 1996; Shimizu et al., 1995; Kimmel et al., 1994; Hertzler and Clark, 1992; Watt and Smith, 1989). Important to the latter two functions (Zhao et al., 1999), are cleavage plane orientation, which may be determined by the long axis of the cell (Rappaport, 1996; Bjerknes, 1986) or by a tissue- or embryo-level reference system (Sausedo et al., 1997; Chenn and McConnell, 1995; Shimizu et al., 1995; Hertzler and Clark, 1992). Although these patterns of cleavage plane orientation are often called random and oriented division, respectively, the more rigorous terms cell-oriented and frame-oriented are used here.

An understanding of mitosis and how it affects and is affected by cell shape and epithelium deformation are important to the development of a comprehensive mechanical understanding of epithelia. For example, during embryo and animal morphogenesis, there are periods of frame-oriented cell division that apparently drive strongly directional in-plane reshaping and, in some cases, are closely correlated with periods of anisotropic cell shape (Zhao et al., 1999; Shimizu et al., 1995; Kimmel et al., 1994; Sausedo and Schoenwolf,

*Corresponding author. Tel.: +1-519-888-4567-6211; fax: +1-519-888-6197.

E-mail address: brodland@uwaterloo.ca (G.W. Brodland).

URL: http://www.civil.uwaterloo.ca/brodland.

0021-9290/02/$ - see front matter
PII: S0021-9290(02)00006-4

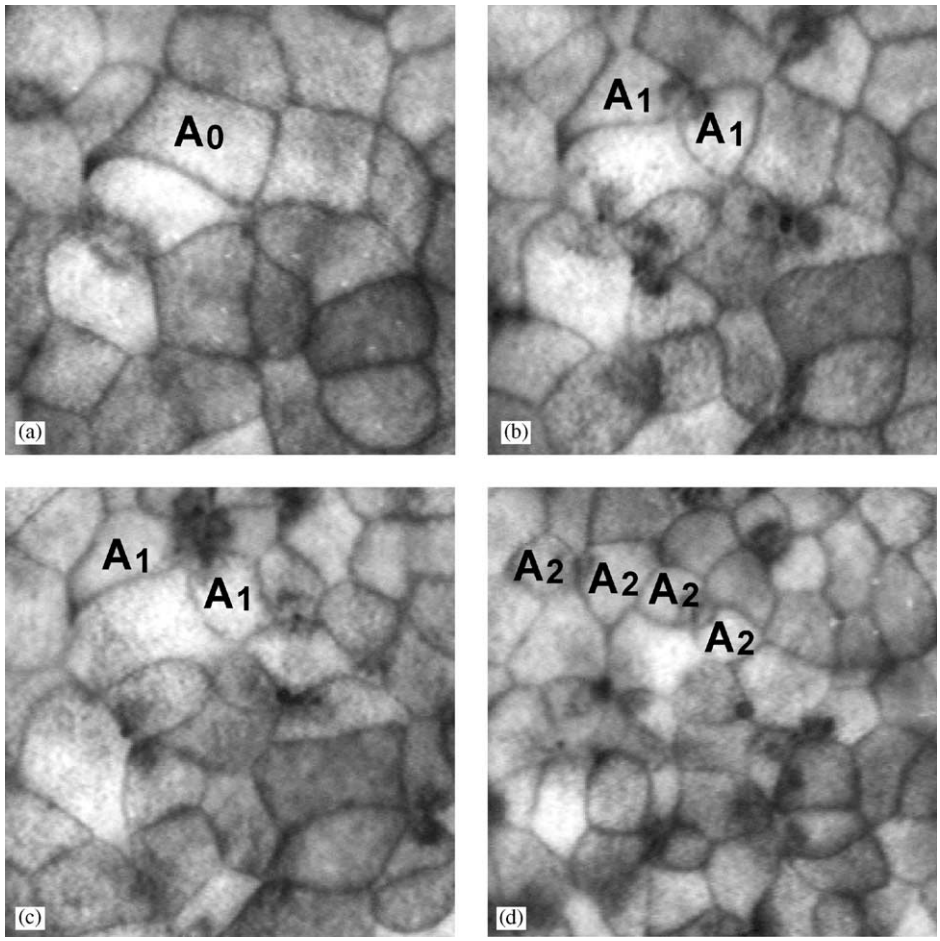

Fig. 1. Mitosis in the dorsal epithelium of a pre-neurulation axolotl (*Ambystoma mexicanum*) embryo. (a) One cell that is on the verge of mitosis, as determined by viewing subsequent images in the series, has been labeled A_0. (b) Fifteen minutes later, mitosis of A_0 is nearly complete, and each of its two forming daughter cells is labeled A_1. (c) Mitosis is complete by 30 min following part (a) of the figure. (d) After an additional 85 min, many more cells have divided including both of the cells labeled A_1 in part (c); they have divided to form four new cells, labeled A_2. Successive cell divisions, such as those that produce the cells labeled A_2, are approximately synchronized with each other (Alberts et al., 1998; Hertzler and Clark, 1992). By part (d) of the figure, all of the cells have undergone at least one division compared to part (a), and since the axolotl does not grow at this early stage of development, the average cell size is significantly reduced.

1993). The causal connections between these phenomena are not yet clear. However, there are indications that embryonic electric fields (Shi and Borgens, 1995; Borgens and Shi, 1995; Jaffe and Stern, 1979) may play a role in establishing cleavage plane orientation and other aspects of development (Zhao et al., 1999; Metcalf and Borgens, 1994). During wound healing, epithelia develop long axes that are oriented normal to the wound edge (Kalnins et al., 1995; Honda, 1983). Again, electric fields are present (Chiang et al., 1992), although mitosis rates are relatively low during wound healing (Fenteany et al., 2000; Zhao et al., 1996), and do not seem to play a significant role in wound closure.

These studies raise a number of important questions such as: Can specific patterns of mitosis actually drive the reshaping of epithelia? If so, what rates of mitosis are required to drive particular reshaping rates? How might mitosis change the stresses or cell shapes in an anisotropic epithelium, and how might pre-existing cell shapes affect mitosis? Although it is not currently possible to answer these questions by altering mitosis patterns or rates at will in real epithelia, they can be investigated using computer simulations. Computer simulations (Honda, 1983; Honda et al., 1984; Brodland and Chen 2000a, b; Chen and Brodland, 2000; Brodland et al., 2000), including recent ones that use finite elements to model individual cells and their interactions, have provided an major step in this direction. The role of mitosis, however, has not yet been investigated using finite element-based simulations.

In the present study, finite element-based computer simulations are used to explore mitosis, and how mitosis, cell shape, and epithelia reshaping depend on each other. Various rates and patterns of mitosis are considered, including frame- and cell-oriented configurations with growing and non-growing daughter cells.

Based on the simulations, formulas are derived that quantify these dependencies, and that can be used to evaluate current theories of epithelia reshaping.

2. Formulation

2.1. Fabric parameters

Consider a rectangular region or patch of an epithelium as shown schematically in Fig. 2. The fabric of this patch can be described in terms of its density ρ, defined as the ratio of the sum of the lengths of the boundaries inside the region plus half of the region perimeter, to the area of the region. The perimeter contribution arises from the assumption that a mirror image of the region is present along each of its boundaries and that half of each of the cell edges along the perimeter are assigned to each. To describe cell shape and orientation, an elliptical composite cell is constructed by summing separately the centroidal moments and products of inertia (I_{xx}, I_{yy} and I_{xy}) of the cells in the region and then dividing by the number of cells in the region. The composite cell is that ellipse which has the same moments and product of inertia equal as these averages. The fabric of the region is then described in terms of κ the ratio of the major axis of this composite cell to its minor axis and α the angle ($-\pi/2<\alpha\leqslant\pi/2$) from the horizontal to its major axis.

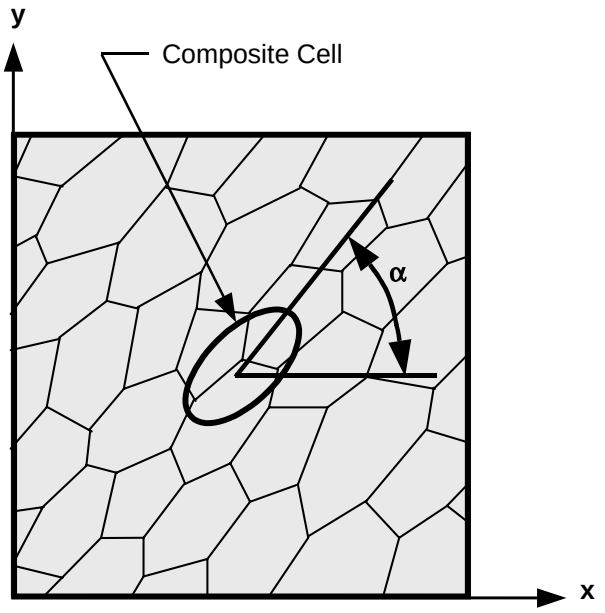

Fig. 2. Parameters that describe the fabric of the epithelium. A "composite" elliptical cell is defined using the moments and products of inertia of the individual cells in the rectangular patch. See text for details. The angle to the long axis of this composite cell is called α and the ratio of its maximum to minimum axes gives the shape parameter κ.

Collectively, κ, α, and ρ provide a robust set of parameters that describe the fabric of an epithelium at any instant.

2.2. Finite element formulation

The computer simulations reported here are based on the finite element formulation of Chen and Brodland (2000), a model has been tested extensively and used to investigate a number of phenomena including tissue engulfment and cell sorting (Brodland and Chen, 2000a). The main features of that formulation are that the forces generated by circumferential microfilament bundles, apical mats of microtubules, contraction of the cell membrane and its associated proteins, cell–cell adhesions and by any structures that produce driving forces are resolved into an equivalent interfacial tension γ (Brodland and Chen, 2000b; Chen and Brodland, 2000). This approach is consistent with the well-established finite element concept of equivalent joint loading, and provides a reliable first approximation to the effects of these driving forces. This approach has the added advantage of condensing the plethora of driving forces into a single parameter. A constant-force, rod-like finite element (Fig. 3) is used to generate the force γ. To model the cytoplasm with its embedded networks of intermediate filaments and organelles, each n-sided cell is divided into n triangular elements area elements, each of which is assumed to have a viscosity μ. Interactions between the cells in the epithelium and their basement membrane are also assumed to be embodied in μ. At the strain rates (of the order of 10^{-4}/s) characteristic of morphogenesis, this seems to provide a satisfactory approximation (Chen and Brodland, 2000). In real cells, the cytoplasm would be free to move from one sector of a cell to another but not from cell to cell. This behavior is embodied in the model by setting Poisson's ratio to

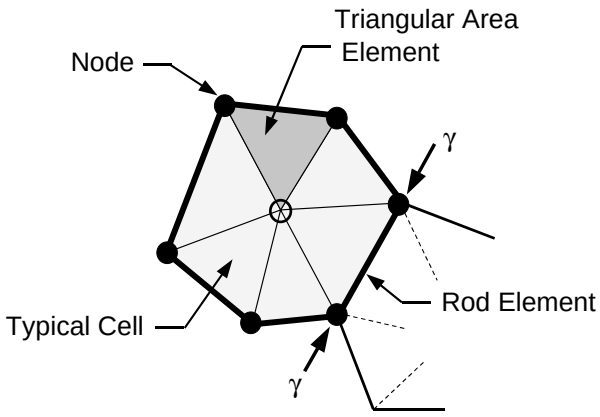

Fig. 3. The finite element model. A typical n-sided cell (shown shaded) is divided into n triangular area elements. The net edge tension γ is applied using a rod-like element that carries a constant tension γ and that has a stiffness of zero.

zero for each triangular element and by imposing a volume constraint on each cell using one Lagrange multiplier per cell. If the cytoplasm in each triangular element had been made incompressible, instead, the volume of each such element would not be free to change as it should. To accommodate cell rearrangement, it is assumed that if the length of the boundary between two cells becomes less than a certain threshold $L_{\min}$, then those two cells become separated while the two cells that were at the ends of this short side come into contact. The newly formed contact is assumed to have a length of $1.1L_{\min}$, so that it does not become targeted for further rearrangement during the next time step (Chen and Brodland, 2000).

To incorporate mitosis into the computer model, a number of modifications were added to the program. These were designed to address the following issues:

1. the rate of cell division,
2. which cells are identified for mitosis in any time step,
3. the orientation of the cleavage plane,
4. the relative size of the two daughter cells,
5. whether or not the daughter cells grow, and if so, how quickly.

The rate of cell division M is defined as the fraction of the current number of cells that divide per unit dimensionless time τ, where τ is defined by

$$\tau = \frac{\gamma \rho t}{2\mu\delta}, \tag{1}$$

where δ is the thickness of the epithelium, and t is the time. Inasmuch as annealing is the fundamental behavior of cells in a patch, the time constant for annealing provides a natural basis for the nondimensionalization of time (Brodland and Chen, 2000a), as in Eq. (1). An analysis of time lapse images of early stage axolotl embryos showed that M can remain sensibly constant over a period of time in which the total number of cells increases by a factor of 8, the length of time for which data were available (four measurements on each of two embryos yielded $M \cong 0.01$). At the beginning of each time step in the simulations, M was used to estimate the number of cell divisions that should occur during that time step. The actual number of divisions is an integer p found by subtracting the number of divisions that have occurred to that point from the accumulated predicted number of divisions, which is stored as a real number. Since the number of divisions in each time step is based on the current number of cells, it increases as the simulation proceeds. If the daughter cells do not grow to the size of their mother cell, ρ increases and the number of divisions per time step increases even more as the simulation proceeds. To identify which cells divide, the p largest cells are chosen, except that no daughter cell may divide again until all other daughter cells have reached the same number of generations as it has.

In cell-oriented division, the cleavage plane was set normal to the long axis of the cell, while in frame-oriented division its direction was specified in the input file. It was positioned to pass through the centroid of the cell, subject to occasional adjustment so that the new triple junctions created by mitosis did not impinge on any pre-existing triple junctions. Finally, a flag was set in the input file to specify whether or not divided cells grew to the area of their mother cell, and a parameter was used to specify the rate at which such growth would occur.

The present model has a number of similarities to that used by Honda et al. (1984). In both, moments of inertia define the long axis of the cell, cell division is assumed to occur by addition of a cleavage plane across the cell, and subsequent reshaping is driven by edge contractions. Honda et al. shows that the cellular patterns predicted by the model are consistent with those that occur in real cells. In real epithelia, the apical ends of the cells may draw in during the early stages of mitosis (Korn and Korn, 1971). Tests in which the model was modified so that the apical area of dividing cells was briefly drawn down to 25% of their original areas just prior to mitosis to simulate this process showed that it made no meaningful difference to the results.

3. Results

3.1. Cell-oriented mitosis

Fig. 4(a) shows an initial configuration of 50 cells made by annealing a Voronoi tesselation (Chen and Brodland, 2000). Such a configuration is similar to that found in real epithelia (Honda, 1983), and was used as the starting configuration for all simulations, unless noted otherwise. For the first simulation, the mitosis rate was set to $M = 0.02$ and, for the purpose of illustration, the first five divisions were specified manually (Fig. 4(b)). The most recently divided cell pair (labeled with the number 5) appears as a bisected mother cell. Immediately thereafter, contraction of the new boundary, in balance with contraction forces in the other nearby boundaries, causes modest localized displacements that round up the cells and restore equilibrium. This local annealing process can be accompanied by cell rearrangement. Soon, the daughter cells become indistinguishable from the older surrounding cells, except perhaps by their slightly smaller size. In this simulation, the time step was chosen so that initially, one division occurred every two time steps. Fig. 4(c) shows the sheet after each of the original cells has dividing once.

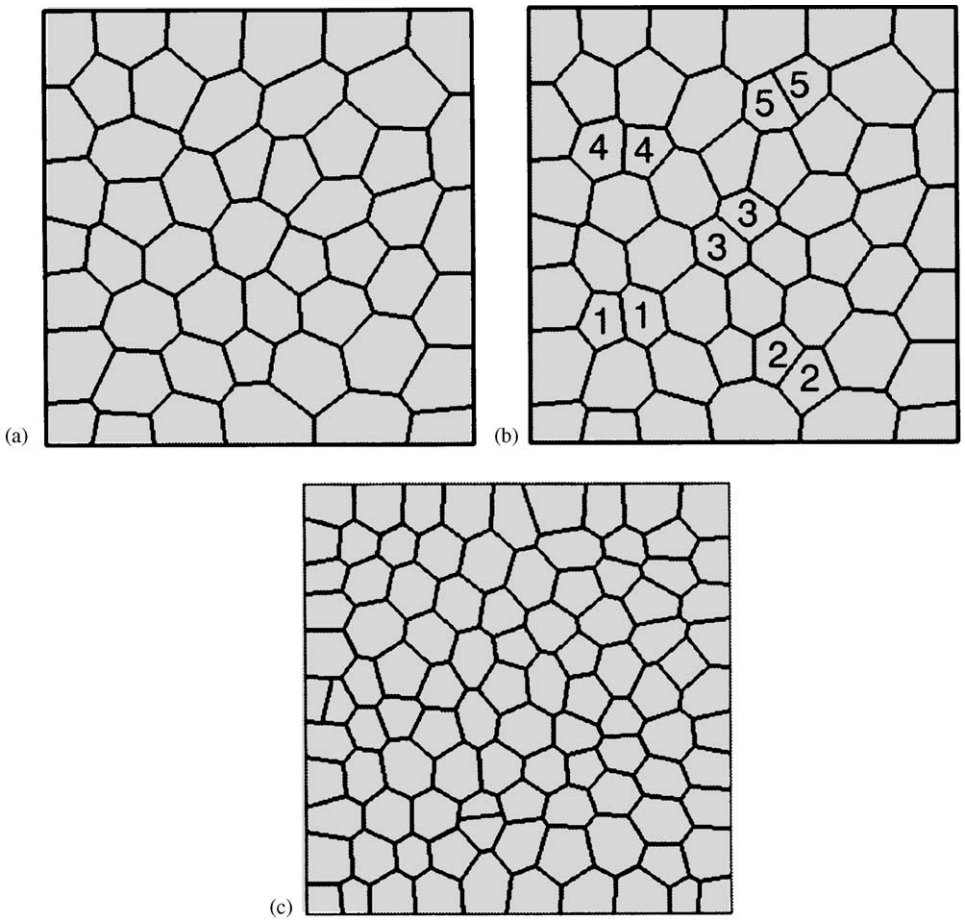

Fig. 4. An isotropic patch undergoing cell-oriented mitosis. (a) Initial configuration. (b) Five manually selected cells have divided. Pairs of daughter cells are numbered in the order in which they came into being. (c) The number of cells has doubled.

Mitosis can also have a dramatic effect on the density parameter ρ, if cells do not grow following mitosis, because the amount of cell boundary is increased. The resulting density can be estimated quite accurately using the somewhat intuitive formula

$$\rho = f\sqrt{\frac{n}{A}}, \tag{2}$$

where A is the patch area (which does not change if the cells do not grow), n is the total number of cells in the patch and f is a form factor that the simulations show has an approximate value of 1.92 for isotropic patches, even if they contain a modest range of cell sizes like those shown here. The value of κ affects f slightly, causing it to rise to $f = 1.97$ when $\kappa = 2$, as in the case considered below. Note that Eq. (2) is general and applies whether or not the cells grow following mitosis and, indeed, whether or not they are undergoing mitosis. Over the course of this simulation, the density ρ increased from 0.0136 to 0.0192 (Eq. (2) predicts a final value of 0.0193) while the composite cell shape κ did not change significantly from its initial value just above unity, and the region remained so nearly isotropic that the composite cell angle α was not meaningful.

To investigate the effect of mitosis on an anisotropic region, the configuration shown in Fig. 4(a) was stretched by multiplying the x-component of each node by 1.90. The result was a patch (Fig. 5(a)) for which $\kappa = 2.0$ and $\alpha = 1.1^\circ$. The mitosis rate was set to $M = 0.125$ and by $\tau = 5.4$, each of the original cells had divided (Fig. 5(b)), while κ had dropped to 1.05 (Fig. 6). Note that the relationship between τ and t changes since the density ρ increases as new cells are formed. Over the range of Fig. 6, the ratio $\Delta\tau/\Delta t$ changes by 44%. This differs only slightly from the theoretical estimate of $\sqrt{2} - 1 = 41\%$ which is based on the fact that the number of cells and thus the number of cell boundaries in any direction increases by approximately $\sqrt{2}$. Additional simulations (not shown), based on a number of different starting configurations, show that the variations between patches are small enough that reliable inferences can be made from a single, 50-cell simulation. In these simulations, a relatively high mitosis rate was chosen on purpose so that the $\kappa-\tau$

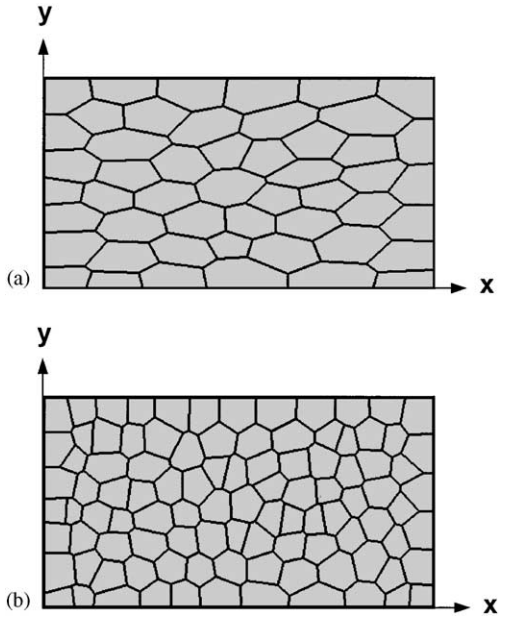

Fig. 5. An anisotropic patch undergoing cell-oriented mitosis. (a) Initial configuration. (b) The number of cells has doubled.

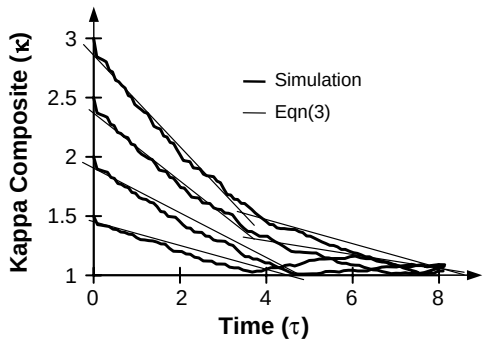

Fig. 6. The effect of mitosis on the cell shape parameter κ. Cell patches had initial composite cell shapes of $\kappa = 1.5$, 2.0, 2.5 and 3.0, and $M = 0.125$. Also shown, are corresponding lines based on Eq. (3).

curve would be governed by mitosis, rather than cell annealing. That boundary contractions played a minor role is evidenced by the relatively large number of newer looking daughter pairs in Fig. 5(b) as compared to Fig. 4(c), both of which show their patches after the number of cells has doubled. In this case, cell-oriented and frame-oriented divisions would both give cleavage planes that are essentially parallel to the y-axis, and observations of the cleavage planes would not be sufficient to identify which was acting.

Here, mitosis causes the shape parameter κ to decrease in an approximately linear way with respect to τ, as shown in Fig. 6. The $\kappa-\tau$ relationship arises from the interaction of several nonlinear phenomena and there does not seem to be a theoretical basis for the linearity of the relationship, although the many simulations that were carried out suggest that this is typical. Since the parameter κ is defined as the ratio of a maximum moment of inertia to a minimum moment of inertia it cannot fall below a value of 1. The slope of the $\kappa-\tau$ relationship depends on the mitosis rate M and on the shape of the largest cells, since those are the ones currently dividing. Thus, if an epithelium starts with $\kappa = 3$ (Fig. 6), those cells with an individual shape parameter $\kappa = 3$ will divide to produce new cells having $\kappa = 1.5$, approximately. These will then divide later, when the original cells have all divided once, and will produce a region that begins at $\tau \cong 4$ and for which the slope is the same as that for a patch that began with $\kappa = 1.5$ (Fig. 6).

On the basis of this understanding, it is possible to derive an approximate relationship

$$\frac{d\kappa}{d\tau} = \phi M(\kappa_{\text{dividing}} - \kappa_{\infty}), \tag{3}$$

where κ_{dividing} is the shape parameter of the individual cell(s) currently dividing, $\kappa_{\infty} = 1$, and ϕ is a scale factor. Using Eq. (3) and typical slopes from the simulation results shown in Fig. 6, it is possible to determine that $\phi \cong -1.6$, and to plot the resulting family of line segments on the figure. Additional tests were carried out to verify that Eq. (3) with $\phi \cong -1.6$ describes the $\kappa-\tau$ relationship for other values of M provided that M is high enough that cell annealing does not contribute significantly to reduction of κ.

To maintain the cell shapes shown in Fig. 5(a) would require significant tension in the x-direction or compression in y (Chen and Brodland, 2000; Brodland et al., 2000). Because mitoses in an anisotropic sheet reduce the degree of cell anisotropy, they also relieve the stresses in the sheet. In this case, by the time the number of cells has doubled (Fig. 5(b)), the stresses in sheet are reduced to 6% of their original values because of the change in average cell shape that occurs. This is consistent with previous studies (Chen and Brodland, 2000; Brodland et al., 2000) that have shown that average cell shape and orientation are primary determinants of the stresses in a cell sheet.

3.2. Cell-oriented mitosis and growth

In some epithelia, mitosis is followed by growth of the daughter cells until they each reach the approximate size of their mother cell. To investigate the effect of cell growth, a simulation was run with $M = 0.01$, a step size of 0.5τ, and with daughter cells that grew to the size of their mother cell over a period of $\tau = 5$. The initial configuration was the same as that shown in Fig. 4(a), and its outline is shown dotted in Fig. 7. The figure also shows the patch after the number of cells has doubled. The final patch is rectangular in shape since the top and right boundaries of the patch were allowed to translate, but not rotate. At this point, the patch is stretched in the x- and y-directions by factors of $\lambda_x = 1.496$ and $\lambda_y = 1.319$, respectively. The resulting area is just less than

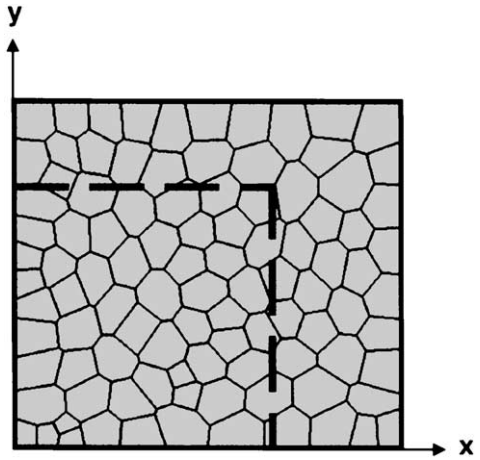

Fig. 7. Cell-oriented mitosis with growth. The cell patch grows in an isotropic manner.

twice the original area because some of the cells have not completed their growth cycles. The difference between λ_x and λ_y in this simulation is uncharacteristically large, and apparently is due to random effects. Also, since no growing or recently divided cells are assumed to be present at the beginning of the simulations, a short transition period occurs. Its effect is usually negligible, although the calculations in the next section were based on steady state values because these produced slightly better correlations.

3.3. Frame-oriented mitosis

To investigate frame-oriented mitosis and growth, a series of simulations, like that shown in Fig. 8, were carried out with M ranging from 0.005 to 0.02, with daughter cell growth being completed within periods ranging from 5 to 20τ, and without daughter cell growth. In these simulations, the cleavage plane was set parallel to the x-axis. The simulations showed that by the time the number of cells doubled, the aspect ratio of all such patches had become 1.99 ± 0.02 or nearly double. If the daughter cells grow, the patch area also doubled during this period of time. This result can be summarized in two pairs of equations for the stretches λ_x and λ_y produced by frame-oriented mitosis with and without growth. In the absence of growth,

$$\lambda_x = \left(1 + \frac{n_d}{n_0}\right)^{-1/2} \tag{4}$$

and

$$\lambda_y = \left(1 + \frac{n_d}{n_0}\right)^{1/2}, \tag{5}$$

where n_0 is the initial number of cells and n_d is the total number of cell divisions. If all cells have divided once, $n_d = n_0$, and if all cells have divided twice, the total number of divisions is $n_d = 3n_0$, since each of the

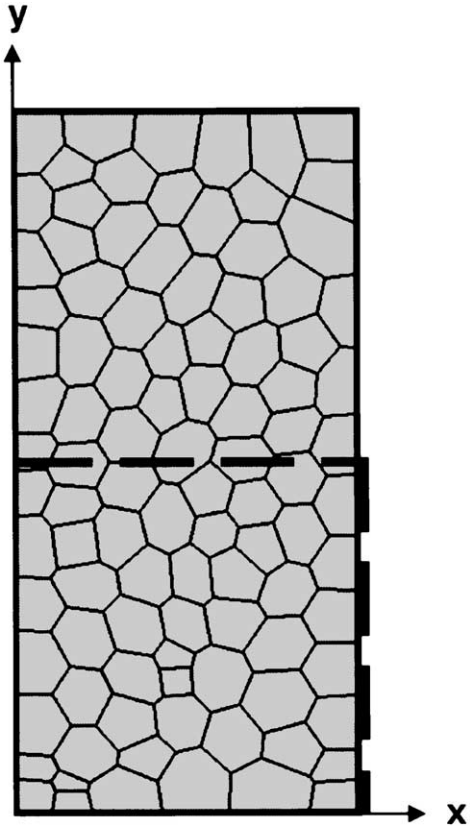

Fig. 8. Frame-oriented mitosis with growth. The patch elongates in the direction normal to the cleavage planes.

original cells divided once and each of the daughter cells also divided once. In the presence of growth, the area simultaneously increases by a factor of $(1 + n_d/n_0)$ in each direction and λ_x and λ_y are found by multiplying Eqs. (4) and (5) by the square root of this factor to give

$$\lambda_x = 1 \tag{6}$$

and

$$\lambda_y = \left(1 + \frac{n_d}{n_0}\right). \tag{7}$$

Both sets of formulas imply that as the rate of frame-oriented divisions increases, the rates of aspect ratio change increase proportionately. In the presence of daughter cell growth, the rate of narrowing produced by reshaping just balances the growth-induced widening. This curious result holds even for slowly growing cells—they take longer to reach full size, but as a result, more of them are growing at any instant.

Fig. 8 shows a simulation that is based on the same parameters as Fig. 7, but with all cleavage planes parallel to the x-axis. After the number of cells has doubled, $\lambda_x = 0.990$ and $\lambda_y = 1.998$, compared with Eqs. (6) and (7) which predict $\lambda_x = 1.000$ and $\lambda_y = 2.000$. As is typical, the cells are nearly isotropic ($\kappa \cong 1$).

4. Discussion

These simulations demonstrate that significant interdependencies can occur between mitosis, cell shape and epithelia reshaping. For example, the simulations show that pre-stretching of a sheet produces cells that have their long axes aligned with the direction of principal stretch, and that this can cause alignment of the resulting cleavage planes (Fig. 5). If such an epithelium is then constrained around its edges, mitosis can produce significant cell reshaping (Fig. 6) and considerable stress relief. To perpetuate the same pattern of cleavage plane orientation would require stress fibers or some other force to deform the daughter cells so that their long axis is in the same direction as that of the mother cell. This would apparently require transient but relatively high stress fiber forces and shortening rates, and sophisticated control, and may explain why few mitoses occur during wound healing. These simulations also demonstrate that cell-oriented mitosis in pre-oriented cells may be essentially indistinguishable from frame-oriented patterns.

Simulations in which the cleavage planes are aligned show that mitoses can drive significant reshaping of an unconstrained epithelium (Fig. 8) or produce considerable stresses in one that is constrained (Brodland et al., 2000). Reshaping occurs in the unconstrained case because of the new, oriented cell boundaries that form. Shortening of these boundaries as the cells round up causes localized narrowing, and because of area constancy in the cells, a concomitant elongation in the opposite direction. It is noteworthy that frame-oriented division is so efficient, with cell doubling producing nearly doubling of the aspect ratio. This reshaping can be accurately predicted by Eqs. (4)–(7). A feature of these formulas is that all necessary parameters for any region can be obtained by counting the initial and final numbers of cells in time-lapse images and comparing cell patch sizes. The simulations also indicate that an initial patch of 50 cells is sufficient for such calculations.

To apply these formulas to a particular biological situation, a patch of at least 50 cells must be used. The number of cells present and the dimensions of the patch could be determined at two different times. The difference in the number of cells indicates the number of cell divisions. From this, the cell division ratio n_d/n_0, and the stretches λ_x and λ_y given by the ratios of the new to old dimensions in corresponding directions are calculated. Since only dimensionless ratios are used in the Eqs. (4)–(7), it is not necessary to determine the scale of any micrographs used nor to define specific counting regions provided that the two regions chosen and the scales used are consistent. It is also not necessary to know the time interval between them. Eqs. (5) and (7) are then used to calculate the amount of stretch in each direction that oriented mitosis would be expected to contribute. As noted below, adjustments may be required if the mitoses are not perfectly frame-aligned. If stretch ratios higher than those predicted by Eqs. (5) and (7) are present, additional driving forces must be present. If lower rates occur, resisting forces must be acting. Such forces could be produced by stresses along the edges of the patch boundary, by stress fibers on the surface of the epithelium, or by other means.

For example, during formation of the zebrafish nervous system, the axial distances between the cells shown in Fig. 4 of Kimmel et al. (1994) increase by a factor of approximately $\lambda_y = 2.74$ between the ends of cell cycles 15 and 16. Assuming no growth of daughter cells, Eq. (5) with $n_d = n_0$ predicts that oriented mitosis would generate an elongation of $\lambda_y = 1.4$. The other approximately half of the observed elongation must be produced by the oriented intercalations that they identify, or by other factors.

Eqs. (4)–(7) are based on the assumption that all cleavage planes are perfectly aligned with the x-axis. It is not difficult to imagine how these equations could be modified to account for cases where this is not the case. If all planes were along a skewed axis, Eqs. (4)–(7) could be applied normal to the skewed axis, and stretch transformation techniques used to convert these stretches to any other axis system. If the axes of the cleavage planes varied from one cell to another, this technique could be applied one division at a time. In practice, it would probably be sufficient to approximate a given angular distribution of cleavage plane orientations by assuming that a certain number of divisions are perfectly frame-oriented while the balance are isotropically distributed. Also, if stresses act along the boundary of the patch, the additional deformations they produce could be calculated (Brodland et al., 2000).

In conclusion, the present study has demonstrated through computer simulations that significant interactions occur between mitosis, average cell shape and epithelium reshaping. It has also produced formulas that describe these dependencies accurately and that can be used to evaluate hypotheses about the role of mitosis in cell and epithelium reshaping.

Acknowledgements

This research was funded by a Research Grant to GWB from the Natural Sciences and Engineering Research Council of Canada (NSERC).

References

Alberts, B., Bray, D., Johnson, A. et al., 1998. Essential cell biology. Garland Publishing Inc., New York.

Beebe, D.C., Masters, B.R., 1996. Cell lineage and the differentiation of corneal epithelial cells. Investigative Ophthalmology and Visual Science 37, 1815–1825.

Bjerknes, M., 1986. Physical theory of the orientation of astral mitotic spindles. Science 234 (12), 1413–1416.

Borgens, R.K., Shi, R., 1995. Uncoupling histogenesis from morphogenesis in the vertebrate embryo by collapse of the transneural tube potential. Developmental Dynamics 203, 456–467.

Brodland, G.W., Chen, H.H., 2000a. The mechanics of heterotypic cell aggregates: insights from computer simulations. ASME Journal of Biomechanical Engineering 122, 402–407.

Brodland, G.W., Chen, H.H., 2000b. The mechanics of cell sorting and envelopment. Journal of Biomechanics 33, 845–851.

Brodland, G.W., Veldhuis, J.H., Chen, D., 2000. How cell shape affects the stresses in a cell sheet. In: Conway, T.A. (Ed.), ASME International Mechanical Engineering Congress and Exposition, Advances in Bioengineering, BED Vol. 48, Orlando, November 5–10, 2000, pp. 79–80.

Burnside, M.B., Jacobson, A.G., 1968. Analysis of morphogenetic movements in the neural plate of the newt *taricha torosa*. Developmental Biology 18, 537–552.

Chen, H.H., Brodland, G.W., 2000. Cell-level finite element studies of viscous cells in planar aggregates. ASME Journal of Biomechanical Engineering 122, 394–401.

Chenn, A., McConnell, S.K., 1995. Cleavage orientation and the asymmetric inheritance of notch1 immunoreactivity in mammalian neurogenesis. Cell 82, 631–641.

Chiang, M., Robinson, K.R., Vanable, J.W., 1992. Electric fields in the vicinity of epithelial wounds in the isolated bovine eye. Experimental Eye Research 54, 999–1003.

Clausi, D.A., Brodland, G.W., 1993. Mechanical evaluation of theories of neurulation using computer simulations. Development 118, 1013–1023.

Fenteany, G., Janmey, P.A., Stossel, T.P., 2000. Signaling pathways and cell mechanics involved in wound closure by epithelial cell sheets. Current Biology 10, 831–838.

Hertzler, P.L., Clark, W.H., 1992. Cleavage and gastrulation in the shrimp *Sicyonia Ingentis*: invagination is accompanied by oriented cell division. Development 116, 127–140.

Honda, H., 1983. Geometrical models for cells in tissues. International Review of Cytology 81, 191–248.

Honda, H., Yamanaka, H., Dan-Sohkawa, M., 1984. A computer simulation of geometrical configurations during cell division. Journal of Theoretical Biology 106, 423–435.

Jaffe, L.F., Stern, C.D., 1979. Strong electric currents leave the primitive streak of chick embryos. Science 206, 569–571.

Kalnins, V.I., Sandig, M., Hergott, G.J., Nagai, H., 1995. Microfilament organization and wound repair in retinal pigment epithelium. Biochemistry and Cell Biology 73, 709–722.

Kimmel, C.B., Warga, R.M., Kane, D.A., 1994. Cell cycles and clonal strings during formation of the zebrafish central nervous system. Development 120, 265–276.

Korn, R.W., Korn, E.O., 1971. Contemporary Perspectives in Biology. Wiley, New York.

Lydon, R.F., 1990. Plant Development: the Cellular Basis. Unwin Hyman, London.

Metcalf, M., Borgens, R.B., 1994. Weak applied voltages interfere with amphibian morphogenesis and pattern. The Journal of Experimental Zoology 268, 323–338.

Rappaport, R., 1996. Cytokinesis in Animal Cells. Cambridge University Press, Cambridge, UK.

Sausedo, R.A, Schoenwolf, G.C., 1993. Cell behaviors underlying notochord formation and extension in avian embryos: quantitative and immunocytochemical studies. The Anatomical Record 237, 58–70.

Sausedo, R.A., Smith, J.L., Schoenwolf, G.C., 1997. Role of nonrandomly oriented cell division in shaping and bending of the neural plate. The Journal of Comparative Neurology 381, 473–488.

Schoenwolf, G.C., Alvarez, I.S., 1989. Roles of neuroepithelial cell rearrangement and division in shaping of the avian neural plate. Development 106, 427–439.

Shi, R., Borgens, R.B., 1995. Three-dimensional gradients of voltage during development of the nervous system as invisible coordinates for the establishment of embryonic pattern. Developmental Dynamics 202, 101–114.

Shimizu, H., Bode, P.M., Bode, H.R., 1995. Patterns of oriented cell division during the steady state morphogenesis of the body column of hydra. Developmental Dynamics 204, 349–357.

Watt, F.M., Smith, J.C., 1989. Cell shape and vertebrate embryogenesis. In: Stein, W.D., Bronner, F. (Eds.), Cell shape: Determinants, Regulation and Regulatory Role. Academic Press, San Diego.

Way, J.C., Wang, L., Run, J.Q., Hung, M.S., 1994. Cell polarity and the mechanism of asymmetric cell division. Bioessays 16, 925–931.

Zhao, M., Agius-Fernandez, A., Forrester, J.V., McCaig, C.D., 1996. Directed migration of corneal epithelial sheets in physiological electric fields. Investigative Ophthalmology and Visual Science 37, 2548–2558.

Zhao, M., Forrester, J.V., McCaig, C.D., 1999. A small, physiological electric field orients cell division. Proceedings of the National Academy of Sciences USA 96, 4942–4946.